NAP-2013

Ternary Systems for the Liquid Immiscibility Gap Technology

V.I. Lutsyk[1,2,*], A.E. Zelenaya[,†]

[1] *Institute of Physical Materials Science SB RAS, 6, Sakhyanova Str., 670047 Ulan-Ude, Russia*
[2] *Buryat State University, 24a, Smolina str., 670000 Ulan-Ude, Russia*

The computer models for T-x-y diagrams with the mono- and invariant monotectic equilibrium, and monovariant syntectic equilibrium by means of kinematical simulation of phase regions boundaries are considered. The effect of syntectic equilibrium changing for monotectic one is investigated with the material balances visualization.

Keywords: Immiscibility Gap, Phase Diagram, Computer Model.

PACS numbers: 64.70.kd, 81.30.Bx

1. INTRODUCTION

T-x-y diagrams with liquid immiscibility is employed widely for the solution of problem associated with a refractory compounds obtaining (borides, silicides and intermetallides). Besides the well-known flax method with only one solvent, the immiscibility gap method for the metallic systems was offered in the third millennium [1-4]. In this method the synthesis and crystallization of compounds have place on the border of two solvents. As this technology includes many unknown details, computer models of phase diagrams will be a useful tool for the understanding.

Phase diagrams with immiscibility can be calculated and investigated using both thermodynamic methods [5-11] and mathematic ones. The elaboration of the algorithms and attendant software, based on a mathematical description of phase diagrams surfaces, permit to construct the space models of T-x-y diagrams and to investigate them. In this case the set of initial experimental data concerning the type of interaction in the system and the data about surfaces contours are used. The hypothetic data can be applied at the deficiency of such initial information. It allows to solve a problem of phase diagram visualization as the three-dimensional object, and to avoid its fragmentary representation [12-14].

The kinematical method of T-x-y diagrams surfaces description is chosen as the most efficient method [15-16]. Here, the kinematical surface is given by the motion of the forming curve along to the set of directing curves, described by the interpolation polynomials. Such method constructs the surfaces with complex geometrical structure [17], involving the folds, extrema, cuts, saddle points.

Computer templates is convenient to use for the simulation of phase diagrams with immiscibility surfaces, having a great quantity of topological modifications, produced by different arrangements and intersections of monovariant lines and immiscibility surfaces [18-19], and at the degeneration of solidus and solvus surfaces. They can be degenerated either on the prism edge, or on the prism side [20].

2. T-X-Y DIAGRAMS COMPUTER MODELS

Let's consider the models of T-x-y diagrams with mono- and invariant monotectic equilibria and monovariant syntectic equilibriun as an example. The coordinates of binary and ternary points on the surfaces contours are given an initial data at the phase diagrams simulation. The following designation are used: i – immiscibility surface, Q – liquidus, S – solidus, V – solvus, i^r – ruled surfaces formed by the intersection lines of immiscibility surface with liquidus on the one hand and the solidus surface folds or intersection lines of two solidus surfaces on the other hand, Q^r – formed by the monovariant lines of liquidus and the intersection lines of solidus surfaces with the solvus ones, S^r – formed by the intersection lines of solidus surfaces with the solvus ones, V^r – formed by the intersection lines of the solvus surfaces, H – horizontal planes.
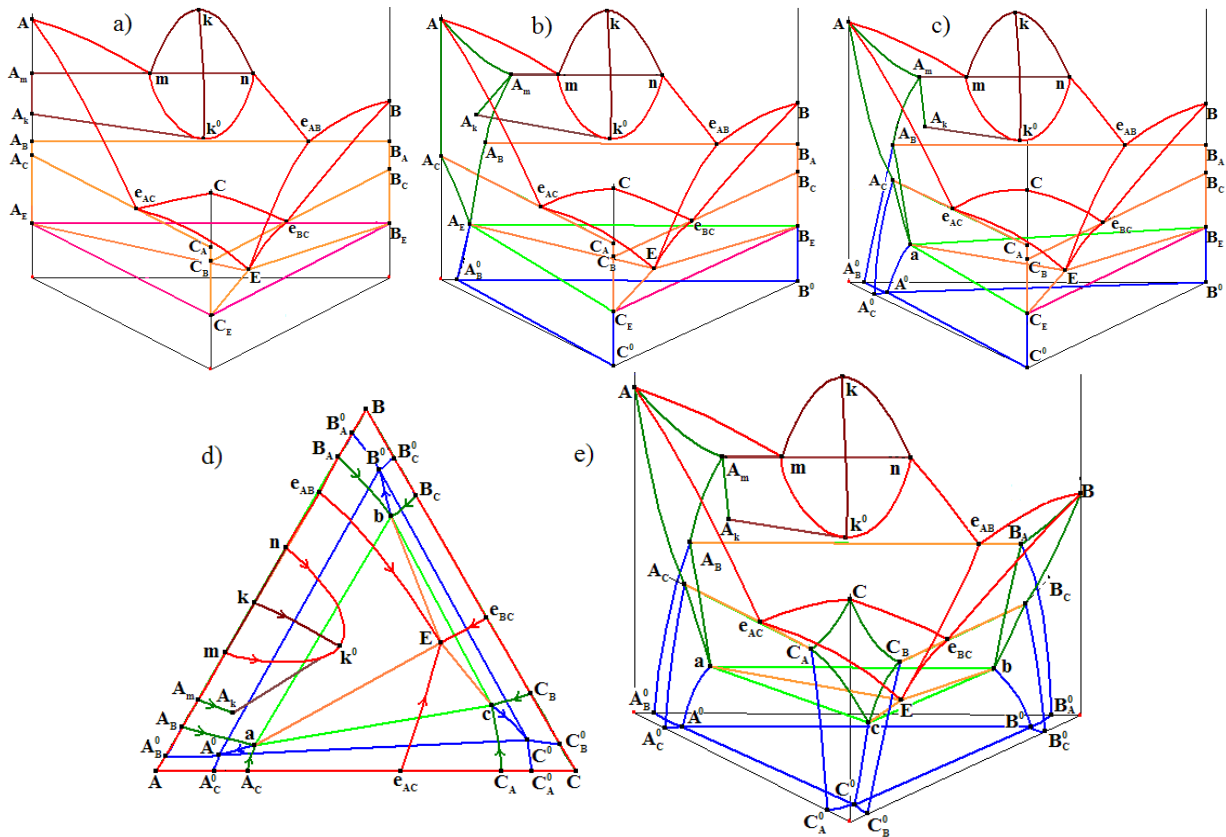
2.1 T-x-y diagram with monovariant monotectic equilibrium

Considered phase diagram without solid solubility is formed by a surface of liquid immiscibility (i: $mknk^0$), 3 liquidus surfaces (Q_A: $Amk^0ne_{AB}Ee_{AC}$, Q_B: $Be_{AB}Ee_{BC}$, Q_C: $Ce_{AC}Ee_{BC}$), 9 ruled surfaces (i^r: $mnkk^0$, i^r_m: $A_mmk^0A_{ko}$, i^r_n: $A_mnk^0A_{ko}$, Q^r_{AB}: $Abe_{AB}EA_E$, Q^r_{BA}: $Bae_{AB}EB_E$, Q^r_{AC}: $Ace_{AC}EA_E$, Q^r_{CA}: $CCae_{AC}EC_E$, Q^r_{BC}: $Bce_{BC}EB_E$, Q^r_{CB}: $Cbe_{BC}EC_E$) and a horizontal complex at invariant eutectic point E (H_E: $A_EB_EC_EE$), consisted of 4 simplexes (Fig. 1a) [16].

The coordinates of initial components (A, B, C), binary eutectic points (e_{AB}, e_{AC}, e_{BC}), a ternary eutectic point (E), points on the contour of immiscibility cupola (k, k^0, m, n) and appropriate points on the edges of prizm (I_{eIJ}, I_E, $I_{m(n)}$, I_{k0} (I=A,B,C)) are taken as the initial data for the phase diagram assemblage. By the use of given computer model we can consider step by step the appearance of solid solubility at one (Fig. 1b-c), two and three components (Fig. 1d-e, Table 1). Fig. 1b-c presents the appearance of solidus and solvus surfaces in component A in binary system AB (Fig. 1b) and both

---
[*] vluts@ipms.bscnet.ru
[†] zel_ann@mail.ru

Fig. 1 – Model of phase diagram with monovariant monotectic equilibrium without (a) and with solid solubility in one (b-c) and three (d-e) components (additional information in Table 1)

binary system A-B and A-C (Fig. 1c). In first case we can see the line of solidus (AA_m, A_mA_B, A_BA_E, A_CA_E, A_mA_k - pseudo-folds) and solvus ($A_EA^0_B$), but second case visualizes the surfaces of solidus ($AA_CaA_BA_m$ with fold A_mA_k) and solvus ($A_Baa^0A^0_B$, $A_Caa^0A^0_C$).

Simulation of solidus and solvus surfaces at all three compounds gives the complete T-x-y diagram with solid phases (Fig. 1d-e). As models come to be more complex, the coordinates of points on the contour of solidus and solvus surfaces are added as initial data of model.

Table 1 – Surfaces within phase diagram with monovariant monotectic equilibrium (view and number) for the different variants of solidus and solvus degeneration (Fig. 1)

Surfaces	a	b	c	d-e
immiscibility surface (i)	1	1	1	1
liquidus surfaces (Q)	3	3	3	3
solidus surfaces (S)	-	4 line in AB binary system	1	3
solvus surfaces (V)	-	1 line in AB binary system	1	6
ruled surfaces of i (i^r)	3	3	3	3
ruled surfaces of Q (Q^r)	6	6	6	6
ruled surfaces of S (S^r)	-	1	2	3
ruled surfaces of V (V^r)	-	1	2	3
horizontal complex (H)	1	1	1	1
Total	14	16	20	29

2.2 T-x-y diagram with invariant monotectic equilibrium

T-x-y diagram (Fig. 2, Table 2) with solid phase solubility includes a surface of liquid immiscibility (i: mMk^0Qnk), 4 liquidus surfaces (Q_A: $AmMe_{AC}$, Q_{A1}: $ne_{AB}EQ$, Q_B: $Be_{AB}Ee_{BC}$, Q_C: $Ce_{AC}Ee_{BC}$), 4 solidus surfaces (S_A: $Am_Ba_Qa_C$, S_{A1}: $m_Ba_Ba_Ea_Q$, S_B: $Bb_{Ab}Eb_C$, S_C: $Cc_{AC}Qc_EC_B$), 6 solvus surfaces (V_{AB}: $ab_Aea^0Ea^0_B$, V_{AC}: $ac_Aqa_Ea^0Ea^0_C$, V_{BA}: $b_Ab_Eb^0Eb^0_A$, V_{BC}: $bc_Bb^0Eb^0_C$, V_{CA}: $c_Ac_Qc_Ec^0Ec^0_A$, V_{CV}: $c_Bc_Ec^0Ec^0_B$), 21 ruled surfaces ($6i^r+8Q^r+4S^r+3V^r$) and 2 horizontal complexes at invariant points E and M(Q). The coordinates of initial components (A, B, C), the binary eutectics (e_{AB}, e_{AC}, e_{BC}), ternary points (E, M, Q), the points of the liquid immiscibility cupola (m, n, k, k^0), the binary and ternary points of the surfaces of the solidus (m_B, a_B, a_C, a_E, a_Q; b_A, b_C, b_E ; c_A, c_B, c_E, c_Q, c_{k0}) and the solvus (a^0_B, a^0_C, a^0_E; b^0_A, b^0_C, b^0_E; c^0_A, c^0_B, c^0_E) were used to understand the surfaces topology.

The peculiarity of this phase diagram is a surface of liquid immiscibility, containing two maximum points (k, k^0) on the edge kk^0 and two minimum points (M, Q) at the same temperature of horizontal complex MQc_Qa_Q. As a solidus surface $Cc_{AC}Qc_EC_B$ has a fold $c_{k0}c_Q$, its contour resemble the contour of the liquidus Q_C, and the adjoining solvus surface $c_Ac_Qc_Ec^0Ec^0_A$ has five points on counter - the same as the solvus surface $ac_Aqa_Ea^0Ea^0_C$.

The use of computer model permits to find the error in the visualization of phase diagrams with liquid immiscibility gap [21]. In [19] the solvus surfaces have
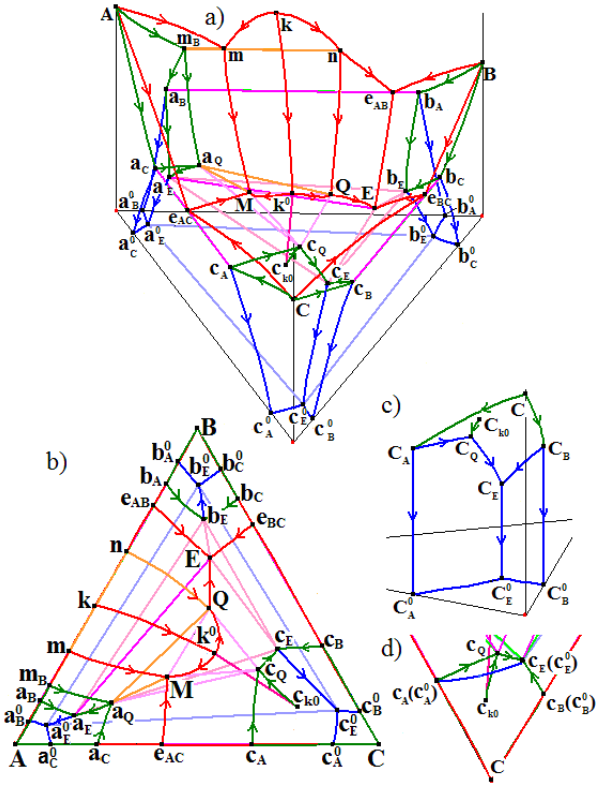
Fig. 2 – 3D model (a) and XY projection (b) of phase diagram with invariant monotectic equilibrium; fragment with orthogonal position of the $L_JL_J^0$ lines on the contour of a solvus surface (c-d)

the orthogonal position of some lines on their contours (Fig. 2c-d – solvus lines CAC0A, CBC0B and CEC0E are projected into the points CA(C0A), CB(C0B), CE(C0E)). At that the projections of solvus surfaces with five points have not the closed contour: line CA(C0A)- CE(C0E) is absent (Fig. 2d).

2.3 T-x-y diagram with monovariant syntectic equilibrium

Given phase diagram has intermediate compound R in the AB binary system (Fig. 3a-b) and forms a surface of liquid immiscibility, 4 liquidus surfaces, 4 solidus surfaces, 10 solvus surfaces, 24 ruled surfaces ($3i^r+10Q^r+5S^r+6V^r$) and 2 horizontal planes at temperatures of the ternary eutectics (E_1 and E_2).

In this case the initial data were the coordinates of the melting points of the initial components (A, B, C), the binary and ternary eutectics (e_{AB}, e_{BA}, e_{AC}, e_{BC}, E_1, E_2, e_r), the points of the liquid–liquid immiscibility cupola (m, n, k, k^0), the binary and ternary points of the surfaces of the solidus (a_B, a_C, a; b_A, b_C, b; c_A, c_B, c_{E1}, c_{E2}, c_r; m_A, n_B, m_{E1}, n_{E2}, r) and the solvus (a^0_B, a^0_C, a^0; b^0_A, b^0_C, b^0; c^0_A, c^0_B, c^0_{E1}, c^0_{E2}, c^0_r; m^0_A, n^0_B, m^0_{E1}, n^0_{E2}, r^0), and the R point of the binary compound. The solidus surface $S_R(m_ARn_Bn_{E2}rm_{E1})$ has the fold RR' (the point R' is located at a temperature corresponding to the lower point k^0 of the liquid immiscibility surface) and point r of a local maximum (Fig. 3c-d). The surfaces of liquidus $Q_R(e_{AB}mk^0ne_{BA}E_2e_rE_1)$ (Fig. 3c) and solidus $S_C(C c_{ACE1}c_rc_{E2}c_B)$ (Fig. 3e) contain the points of maxima e_r and c_r too.
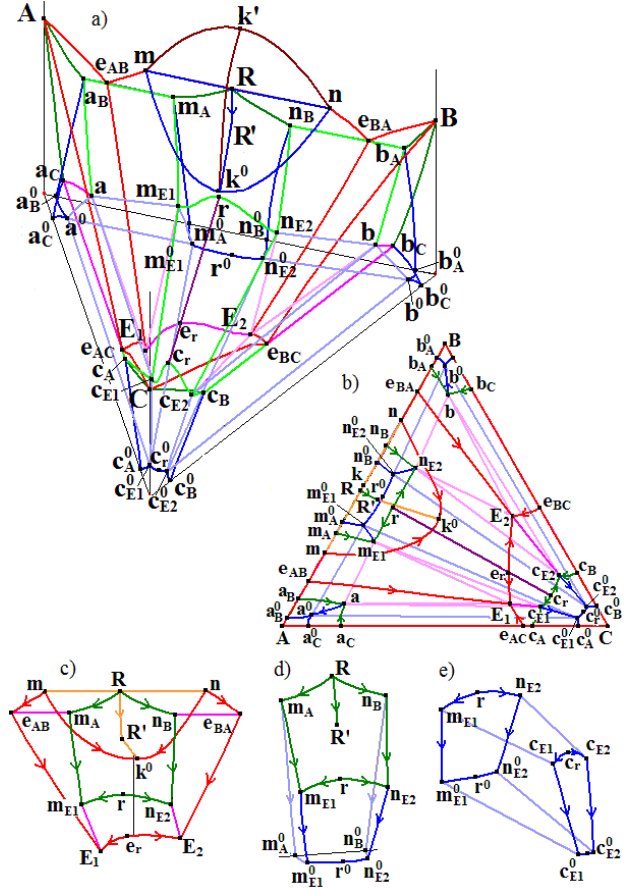

Fig. 3 – 3D model (a) and XY projection (b) of phase diagram with monovariant syntectic equilibrium and phase regions L+R (c), C+R (d) and R (e)

A transition of syntectic equilibrium $L_1+L_2 \rightleftarrows R$ into the monotectic one ($L_1 \rightleftarrows L_2+R$ or $L_2 \rightleftarrows L_1+R$) occurs in the phase region L_1+L_2+R [18, 22-23]. In this case two surfaces of 2-phase reactions $L_1 \rightleftarrows L_2$ and $L_2 \rightleftarrows L_1$ are appeared, and both these surfaces have a common generation segment k^0R' (at the same time it is a tie-line between the $L_1(L_2)$ and R phases (Fig. 4a). Phase region L_1+L_2+R is bounded by three ruled surfaces, i^r (with contour mk^0n), i^r_m (mRR'), i^r_n (nRR'), where the curves mk^0 and nk^0 are the crossing curves of immiscibility and liquidus surfaces.

The diagrams of material balance for arbitrary given mass center make possible to investigate the process of phase reaction type change in more detail. The composition G (0.46; 0.42; 0.12) (Fig. 4b) intersects the ruled surface i^r at T=620.5 and moves from two-phase region L_1+L_2 into three-phase region L_1+L_2+R. In phase region L_1+L_2+R the decrease of phases L_1 and L_2 portions, and the increase of phase R portion take place. At T=571.21 the decrease of phase L_1 portion stops and its increase begins, that is the change of syntectic equilibrium ($L_1+L_2 \rightleftarrows R$) to monotectic one ($L_2 \rightleftarrows L_1+R$) takes place. At T=558.49 point G intersects the ruled surface i^r_m and phase L_2 disappears. Below temperature 558.49 composition G falls into phase region L+R.

One, two or three surfaces of two-phase reaction can appear at the deformation of phase region L1+L2+R in such way that the line RR' is beyond the contour of line mk0n in projection [23]. Usually this surface forms in the area of lines RR' and mk0n intersection. More series deformation of the contour curves will produce two surfaces of two-phase reaction, adjoining to tie-line R'k0.

Table 2 – Surfaces of phase diagram (Fig. 3)

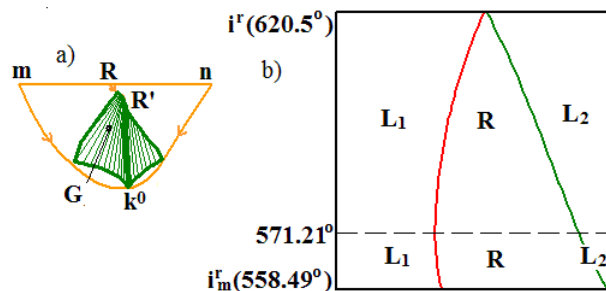| Name	Contour	Name	Contour
i	$mknk^0$	Q^r_{AR}	$e_{AB}a_BaE_1$
Q_A	$Ae_{AB}E_1e_{AC}$	Q^r_{RA}	$e_{AB}m_Am_{E1}E_1$
Q_B	$Be_{BA}E_2e_{BC}$	Q^r_{AC}	$e_{AC}acaE_1$
Q_R	$e_{AB}mk^0ne_{BA}E_2e_rE_1$	Q^r_{CA}	$e_{AC}C_{ACE1}E_1$
Q_C	$Ce_{AC}E_1e_rE_2e_{BC}$	Q^r_{BR}	$e_Ba_ba_bE_2$
S_A	Aa_Ba_C	Q^r_{RB}	$e_{BA}n_Bn_{E2}E_2$
S_B	Bb_Ab_C	Q^r_{BC}	$e_Bc_bc_bE_2$
S_R	$m_ARn_BN_{E2}rm_{E1}$	Q^r_{CB}	$e_{BC}c_BC_{E2}E_2$
S_C	$Cc_{AC}E_1c_rC_{E2}c_B$	Q^r_{CR}	$E_1c_{E1}c_{E2}E_2$
V_{AB}	$a_Baa^0a^0_B$	Q^r_{RC}	$E_1m_{E1}n_{E2}E_2$
V_{AC}	$acaa^0a^0_C$	S^r_{AR}	$a_Bm_Am_{E1}a$
V_{BA}	$b_Abb^0b^0_A$	S^r_{BR}	$b_An_Bn_{E2}b$
V_{BC}	$bcbb^0b^0_C$	S^r_{AC}	$acc_{ACE1}a$
V_{CA}	$c_AC_{E1}c^0E_1c^0_A$	S^r_{BC}	$bcc_{BCE2}b$
V_{CB}	$c_BC_{E2}c^0E_2c^0_B$	S^r_{RC}	$c_{E1}m_{E1}n_{E2}c_{E2}$
V_{CR}	$c_{E1}c_rC_{E2}c^0E_2c^0_rc^0_{E1}$	V^r_{AR}	$am_{E1}m^0_{E1}a^0$
V_{RA}	$m_Am_{E1}m^0_{E1}m^0_A$	V^r_{BR}	$bn_{E2}n^0_{E2}b^0$
V_{RB}	$n_BN_{E2}n^0_{E2}n^0_B$	V^r_{AC}	$ac_{E1}c^0_{E1}a^0$
V_{RC}	$m_{E1}rn_{E2}n^0_{E2}r^0m^0_{E1}$	V^r_{BC}	$bc_{E2}c^0_{E2}b^0$
i^r	mnk^0	V^r_{RCm}	$c_{E1}m_{E1}m^0_{E1}c^0_{E1}$
i^r_m	$mR(R,r)^0$	V^r_{RCn}	$c_{E2}n_{E2}n^0_{E2}c^0_{E2}$
i^r_n	$nR(R,r)^0$	H_{E1}	$ac_{E1}m_{E1}$
		H_{E2}	$bc_{E2}n_{E2}$

Fig. 4 – Surfaces of two-phase reaction for phase region L_1+L_2+R (a); the material balances for the compositions G (b)

5. CONCLUSIONS

Using the mathematical methods of phase diagrams elements descriptions at the computer software allowed to simulate the whole geometrical structure of diagram on the basis of minimal initial information. At that the effectiveness of corresponding physics-chemical systems study is increased: the visualization of diagram geometrical model and its sections has been possible, the founding of information about the results of initial components interaction for the work content reduction of new materials creation has become available. Such software makes possible to solve the problem of heterogeneous materials computer-aided design.

REFERENCES

1. U. Burkhardt., M. Bostrom, W. Schnelle, Z. Hui, Yu. Grin, V. Gurin, *Proc. 9th. European Conf. Solid State Chem.* (Stuttgart, Germany). 204 (2003).
2. U. Burkhardt, V. Gurin, Y. Grin, *Develop. Inst. and Sci. Rep.* (2006).
3. V. Gurin, U. Burkhardt, Yu. Grin, *J. Phys. Conference Series* **175**, 012012 (2009).
4. V.N. Gurin, Yu. Grin'., U. Burkhardt, M.V. Konovalov, *Bull. Russ. Acad. Sci.: Phys.* **73**, 1386 (2009).
5. G. Kaptay, *Calphad* **29**, 56 (2005).
6. D.V. Malakhov, X.J. Liu, I. Ohnuma, K. Ishida, *J. Phase Equilib.* **21**, 514 (2000).
7. S. Zhang, D. Shin, Z.-K. Liu, *Calphad* **27**, 235 (2003).
8. P.-Y. Chevalier, E. Fischer, B. Cheynet, *Calphad* **28**, 15 (2004).
9. J. Vizdal, M.H. Braga, A. Kroupa, K.W. Richter, D. Soares, L.F. Malheiros, J. Ferreira, *Calphad* **31**, 438 (2007).
10. M.-N. Avettand-Fènoël, N. David, G. Reumont, J.-M. Fiorani, M. Vilasi, P. Perro, *J. Therm. Anal. Calorim.* **90**, 329 (2007).
11. A. Shukla, Y.-B. Kang, A.D. Pelton, *Calphad* **32**, 470 (2008).
12. E. Wenda, A. Bielański, *J. Therm. Anal. Calorim.* **93**, 973 (2008).
13. X. Huanga, P. Song, L.Lu.B. Chen, *Calphad* **32**, 188 (2008).
14. S.H. Zhou, Y. Wang, L.-Q. Chen, Z.-K. Liu, R.E. Napolitano, *Calphad* **33**, 631 (2009).
15. V.I. Lutsyk, A.M. Zyryanov, *Mater. Res. Soc. Symp. Proc.* **804**, 349 (2004).
16. V.I. Lutsyk, A.M. Zyryanov, A.E. Zelenaya, *Russ. J. Inorg. Chem.* **53**, 792 (2008).
17. V.I. Lutsyk, A.E. Zelenaya, V.V. Savinov, *IOP Conf. Ser.: Mater. Sci. Eng.* **18**, 112005 (2011)
18. K.A. Khaldoyanidi, *Phazovye diagramy heterogennnykh sistem s transformatsiyami* (Novosibirsk: SB RAS Publ. Comp.: 2004). [In Russian]
19. A. Prince, *Alloy phase equilibria* (Amsterdam-London-N.Y.: Elsevier Publ. Comp.: 1966).
20. R. Vogel, *Die Heterogenen Gleichgewichte* (German: Akademische Verlagsgesellschaft: 1959).
21. V. Lutsyk, A. Zelenaya, V. Vorob'eva, *Abstract of Calphad XXXVIII* 146 (2009).
22. V.I. Lutsyk, V.P. Vorob'eva, A.M. Zyryanov, *J. of Guangdong Non-Ferrous Metals* **15**, 174 (2005).
23. V.I. Lutsyk, A.E. Zelenaya, A.M. Zyryanov, *Crystallogr. Rep.* **54**, p. 1300 (2009).